Plastic Poisson's Ratio of Nanoporous Metals: A Macroscopic Signature of Tension-Compression Asymmetry at the Nanoscale

Lukas Lührs[a], Birthe Zandersons[a], Norbert Huber [b,a], Jörg Weissmüller[a,b]

[a] Institute of Materials Physics and Technology, Hamburg University of Technology, Hamburg, Germany

[b] Institute of Materials Research, Materials Mechanics, Helmholtz-Zentrum Geesthacht, Geesthacht, Germany

Section SOM-I: Details of strain measurement by digital image correlation

Sample deformation during mechanical testing was measured using digital image correlation. Images were taken by a VC-Phantom M110 CCD-Camera equipped with a telecentric objective, configured to provide a large depth of focus. A dedicated illumination system provided uniform illumination and was carefully placed to avoid reflections. A cuvette from optical glass and with planar windows served as the electrochemical cell, minimizing image distortions. In order to minimize refraction effects, the optical path was aligned perpendicular to the front window of the cuvette. Furthermore, a large (≥ 250 mm) object distance ensured essentially normal incidence.

From consecutive grey scale images displacement fields were calculated using the software DaVis 8.2.0 (LaVision®), an exemplary image at initial deformation is shown in **Figure S1**. Strains parallel, $\varepsilon_\parallel$, and perpendicular, $\varepsilon_\perp$, to the load axis were determined by "virtual strain gauges". Virtual strain gauges are pairs of points on the image of the sample surface that are traced by the software, see for instance the colored lines in Fig S1. Their relative displacement provides the strain in the direction of the connection line. Fig S1 shows an example for the location of virtual strain gauges providing $\varepsilon_\parallel$ and $\varepsilon_\perp$ in our experiment. Note that the telecentric objective and the uniform illumination afforded a valid strain measurement even though the image represents a curved area of sample surface.
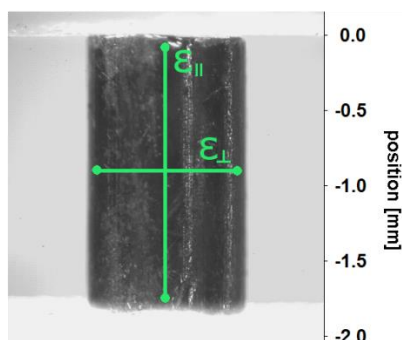
Figure S1: Exemplary grey-value image of a nanoporous gold sample during compression testing in electrolyte. Strain measurements in loading direction $\varepsilon_\parallel$ and perpendicular $\varepsilon_\perp$ to it are depicted schematically by green lines. Image recorded in situ, in the electrochemical cell.

Technical data as well as calculation parameters of the digital image correlation measurement are given in **Table S1**. For a detailed description, addressing the theoretical as well as practical concepts of this type of measurement Ref. [1] is recommended.

Table S1: Technical data and used evaluation parameters of the digital image correlation setup.

Parameter	Value	Parameter	Value
Image acquisition rate	0.2 Hz	Pixel to µm conversion	3-4 µm/pixel
Exposure time	4000-8000 µs	Step size	7-10 pixels
Camera resolution	1280x800 pixel	Subset size	19-40 pixels
Evaluated image section	140000-150000 pixels		

**Section SOM-II: Variation of surface tension during potential jumps**

As is pointed out in the main text of the manuscript, jumps in the electrode potential lead to a substantial variation, $\Delta\gamma$, of the surface tension as a consequence of the electrical work that is associated with charging the surface. This work is embodied in the Lippmann equation, Eq (3) of the main text, and Figs 1(c) and 2 illustrate the results of our experiments exploring $\Delta\gamma$.

In principle, there is also a second effect that changes the value of γ: The surface tension is independent of the *plastic* strain, but *elastic* deformation entails a variation $\delta\gamma = f\delta e$ where f denotes the surface stress (see the classic publication by Shuttleworth, Ref [2]; the distinction between plastic and elastic strain in this context is discussed in detail in Ref [3]) and e is the elastic area strain, relative change in surface area by elastic deformation. Yet, this second effect is negligible: The potential jumps in our experiment entail changes, $\delta\sigma_F$, in flow stress by no more than 50% (see Figs 3(d), 3(f)). According to Fig 5(b), the maximum local flow stress is around 800 MPa, so that $\delta\sigma_F \lesssim 400$MPa. Accounting for the elastic parameters of bulk gold ($Y_B = 80$ GPa, $\nu_B = 0.44$), the axial stress jump by $\delta\sigma_F$ then entails the area strain $\delta e = \delta\sigma_F Y_B^{-1}(1 - \nu_B) \leq 0.002$. Since $f \lesssim 3$ N/m [4], we then find that $\delta\gamma$ due to elastic deformation is no larger than $f\delta e = 0.015$ N/m or around 1% of the absolute value of γ. This change is much smaller than the variation in γ in response to pseudo-capacitive charging, which is estimated as -66% (see Section 3.2). Therefore, the variation in γ due to elastic strain and surface stress has been neglected in our model.

Section SOM-III: Separating contributions of surface tension and work hardening rate to the plastic Poisson's ratio in finite element simulations

In **Figure S2** the individual contributions of switching *i.*) surface tension γ and of *ii.*) work hardening rate E_T^B are displayed separately. Graphs (a) and (b) show that switching of γ on/off while holding E_T^B constant reproduces the significant variation of the plastic Poisson's ratio ν_P of the experiment. The experimental jumps in the flow stress are only partly captured. By contrast, when E_T^B is switched while γ is held constant at 0 (that is $\gamma = $ "off"), graphs (c) and (d), then the experimental jump in flow stress is reproduced but the variation of ν_P is not.

The key observation is: Switching the surface tension but not the work hardening reproduces the experimental jump in ν_P, switching the work hardening but not the surface tension does not. This confirms the notion, in the main text of the paper, that the significant variation of ν_P can be attributed to the action of the surface tension.
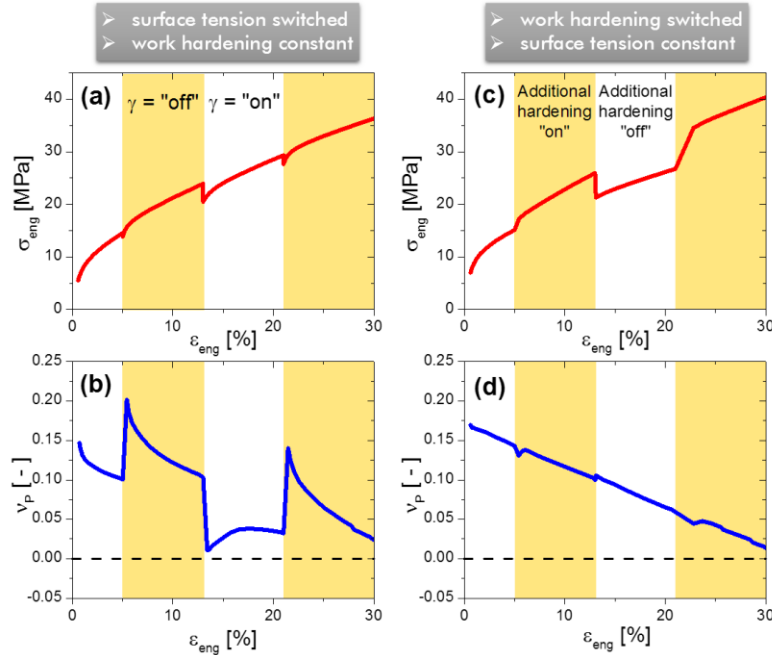
Figure S1: Finite element simulations representing the structure of nanoporous gold with a ligament size of 40 nm. Separated illustration of the influence of surface tension γ and work hardening rate E_T^B on the engineering stress σ_{eng} and plastic Poisson's ratio ν_P, respectively; both plotted vs. the engineering strain ε_{eng}. **(a,b)** Step wise switching of $\gamma = $ "on" and "off" (white and yellow regions, respectively), while E_T^B remains constant at 4 GPa. **(c,d)** γ is set to 0, i.e. switched "off", while E_T^B is switched between 4 GPa (additional hardening "off") and 6 GPa (additional hardening "on") as highlighted in the graph by white and yellow regions, respectively.

References

1. H. Schreier, Orteu J. and Sutton M. A., *Image Correlation for Shape, Motion and Deformation Measurements.* NY, Springer US (2009).

2. R. Shuttleworth, *The Surface Tension of Solids.* Proceedings of the Physical Society of London Section A **63** (1950) 444.

3. D. Kramer and J. Weissmüller, *A note on surface stress and surface tension and their interrelation via Shuttleworth's equation and the Lippmann equation.* Surface Science **601** (2007) 3042.

4. Y. Umeno, C. Elsässer, B. Meyer, P. Gumbsch, M. Nothacker, J. Weissmüller and F. Evers, *Ab initio study of surface stress response to charging.* EPL **78** (2007) 13001.